real

by FAUZAL ZOHEDI

Submission date: 22-Jul-2024 10:55AM (UTC+0800)
Submission ID: 2256655401
File name: Real-Time_1.docx (3.5M)
Word count: 4921
Character count: 26754

SINERGI Vol. xx, No. x, February 20xx: xxx-xxx
http://publikasi.mercubuana.ac.id/index.php/sinergi
http://doi.org/10.22441/sinergi.xxxx.x.xxx

Real-Time Unmanned Surface Robot (USR) for River Quality Monitoring System

Mohd Shahrieel Mohd Aras[1*], Pavitrah Ponusamy[1], Mohamad Riduwan Md Nawawi[1], Fauzal Naim Zolkapli[1], Mohd Bazli Bahar[1], Lokman Abdullah[2], Alias Khamis[1], Zairi Ismael Rizman[3]
[1]Faculty of Technology and Electrical Engineering, Universiti Teknikal Malaysia Melaka, Malaysia
[2]Faculty of Industrial and Manufacturing Technology and Engineering, Universiti Teknikal Malaysia Melaka, Malaysia
[3]School of Electrical Engineering, College of Engineering, Universiti Teknologi MARA, Terengganu, Malaysia

Abstract
A real-time Unmanned Surface Robot (USR) for river water quality monitoring system is a technology that employs a small autonomous boat outfitted with sensors and other monitoring equipment to gather and transmit data on various water quality parameters like pH, temperature and total dissolved solids sensors in rivers and other bodies of water. The USR can traverse the river, gather information or data at specific points or designated locations, as well as continuously monitor a specific stretch of river at all times. The data or information are sent in real time to a central monitoring station, where it is analyzed and used to identify potential water quality problems. First, the USR will be designed using SolidWorks software and investigate and examine the design of USR focusing on the structure performances of USR. Then, this USR will be developed and fabricated. The complete system of USR can provide valuable information for water resource management as well as aid in the detection and mitigation of pollution and other environmental issues. Next, to determine the overall performance of the USR, five experiments and autopilot accuracy tests were performed. Finally, the project also aims to verify and validate the accuracy of water quality monitoring sensors.

Keywords:
Self-navigation;
SolidWorks design;
Unmanned surface robot;
Water quality

Article History:
Received: May 2, 2019
Revised: May 29, 2019
Accepted: June 2, 2019
Published: June 2, 2019

Corresponding Author:
Mohd Shahrieel Mohd Aras
Faculty of Technology and Electrical Engineering, Universiti Teknikal Malaysia Melaka, Malaysia
Email: shahrieel@utem.edu.my

INTRODUCTION

In Malaysia, rivers are the source of 98% of all water consumption [1]. Despite the fact that Malaysia is blessed with many rivers, river pollution prevents the large amount of water resources in the catchment from ensuring a sufficient supply for all users [2, 3, 4, 5]. In general, both point and non-point sources contribute to water pollution in Malaysia. Sewage treatment facilities, manufacturing, agricultural and livestock farms are all examples of point sources. Activities such as logging, land clearing and earthmoving operations are responsible for non-point sources [6]. Existing river water quality monitoring system does not get water samples from different points of the river. The major feature that a river water quality monitoring system requires is the mobility of the system to monitor water in different points of the river.

Furthermore, traditional water quality monitoring methods can be time consuming, expensive and limited in their ability to provide real time data. Also, manual sampling and laboratory analysis may not be feasible in some areas such as remote or heavily polluted areas [7, 8, 9, 10]. The existing real time river water quality system does not provide accurate physicochemical reading of the water. Examples of

physicochemical readings are pH, total dissolved solid, dissolved oxygen and so on. There are several problems associated with motion control of surface robots that can affect their ability to navigate and collect data in rivers and other bodies of water [11, 12, 13]. Maintaining a precise position in the presence of currents, waves and wind is challenging [14]. The surface robot needs to be able to maintain a precise position to collect accurate data, and it must also be able to return to a precise position in case of an emergency. Surface robots need to be able to follow a precise trajectory to collect data on water quality parameters. This can be challenging due to the presence of currents, waves and wind which can cause the surface robot to deviate from its intended trajectory [15, 16, 17, 18, 19].

The purpose of this project is to design and construct an Unmanned Surface Robot (USR) for monitoring river water quality in real-time. In this paper also contained a validation and verification of the water quality monitoring system's accuracy. Additionally, it examines the USR's mobility and stability characteristics. The background research on mechanical design and configuration will be discussed in upcoming part.

Mechanical Design of Unmanned Surface Robot

Table 1 shows comparison of the previous researches and the research gap [20, 21, 22,23]. In this table, comparison flight controller used, type surface robot and the sensor used for every project. Three previous projects will be covered and show the research gap.

Table 1. Comparison of the previous researches and the research gap

Research Title	Project Description	Flight Controller Used	Type of Surface Robot	Accuracy of Sensors	Gap
Autonomous Surface Vehicle for Real-time Monitoring of Water Bodies in Bangladesh	The research used a small autonomous hovering boat to monitor water bodies in Dhaka, Bangladesh.	Arduino Mega	Monohull	The accuracy of the pH sensor reading and Turbidity sensor reading very low	The flight controller used is Arduino Mega which is slower compared to pixhawk fight controller. It also uses Monomial boat will be less stable compared to Catamaran. The accuracy is low as well
Design and Implementation of Unmanned Surface Vehicle for Water Quality Monitoring	The unmanned surface vehicle was designed with enhanced intelligence and maneuverability to monitor river water quality.	ARM Cortex-M3 with an STM32F103ZE	Multihull Catamaran	Accuracy of water quality sensors not mentioned	The ARM Cortex-M3 used is which is slower compared to pixhawk fight controller. The accuracy is of the sensor is not measured in this research
A Design of Radio-controlled Submarine Modification for River Water Quality Monitoring	The flow of domestic, agricultural, and industrial water into rivers prompted the development of the radio-controlled river water quality monitoring submarine.	ARM F4 and Raspberry Pi B+	Submarine	Accuracy of water quality sensors not mentioned	The type of vehicle build in this research is submarine whereas our objective is to build a Surface Robot. The accuracy is of the sensor is not measured in this research

Configuration

Table 2 shows the comparison between single propeller single rudder and twin propeller twin rudder system for the surface robot [24, 25, 26, 27]. Table 3 shows the comparison between types of boat such as airboat, catamaran and sailboat.

Table **Error! No text of specified style in document.**. Comparison between Types of Boat Propeller and Rudder Configuration

Types of Boat Propeller and Rudder Configuration	Advantages	Disadvantages
Single Propeller Single Rudder System	This configuration is simpler and less expensive than a twin rudder twin propeller system, and it can be more efficient in certain situations such as when operating in calm waters or at a steady speed.	This configuration has limited maneuverability. With only one rudder and one propeller, the vessel is less able to

		make tight turns or perform evasive maneuvers.
Twin Propeller and Twin Rudder System	This configuration can provide increased maneuverability and control, as well as redundancy in case of failure. It also allows for independent control of the speed and direction of each propeller, which can be useful in certain situations such as docking or station keeping.	This configuration is more complicated than a single-rudder, single-propeller system and the twin-rudder, twin-propeller system is typically heavier.
Twin Propeller System	Twin propellers provide enhanced maneuverability, allowing the boat to make tight turns and navigate in confined spaces more easily. Each propeller can operate independently, enabling better control over the boat's movement. With two engines, twin propeller boats offer redundancy. If one engine fails or experiences a problem, the other engine can still keep the boat operational and help you reach your destination or return safely to shore.	Win propeller boats generally consume more fuel than single-engine boats due to the increased power and weight. This can result in higher operating costs, especially during long trips or when operating at higher speeds.

Table 2. Comparison between Types of Boats

Type of Boats	Operating Principle	Advantages	Disadvantages
Airboat	Uses a propeller above the boat and maneuver around using wind force	Airboat Favored when a higher level of persistence is required and energy independence is desired	Not suitable for rough water condition. Limited range due to fuel consumption.
Catamaran	Uses rudders to change its direction of movement and an underwater thruster for propulsion.	Increased ability to maneuver and power to resist currents	Higher cost compared to other types of surface robots.
Sailboat	Utilize a sail to convert the wind's energy into a propulsion force.	Can operate with no emissions or fuel consumption. Can navigate through light wind condition	Limited speed and maneuverability compared to motorized vessels.

METHOD

Based on Figure 1, the project flow chart shows the overall project flow from the beginning until the completion of the project and how to proceed if certain conditions are not met. It is used as the project guideline.

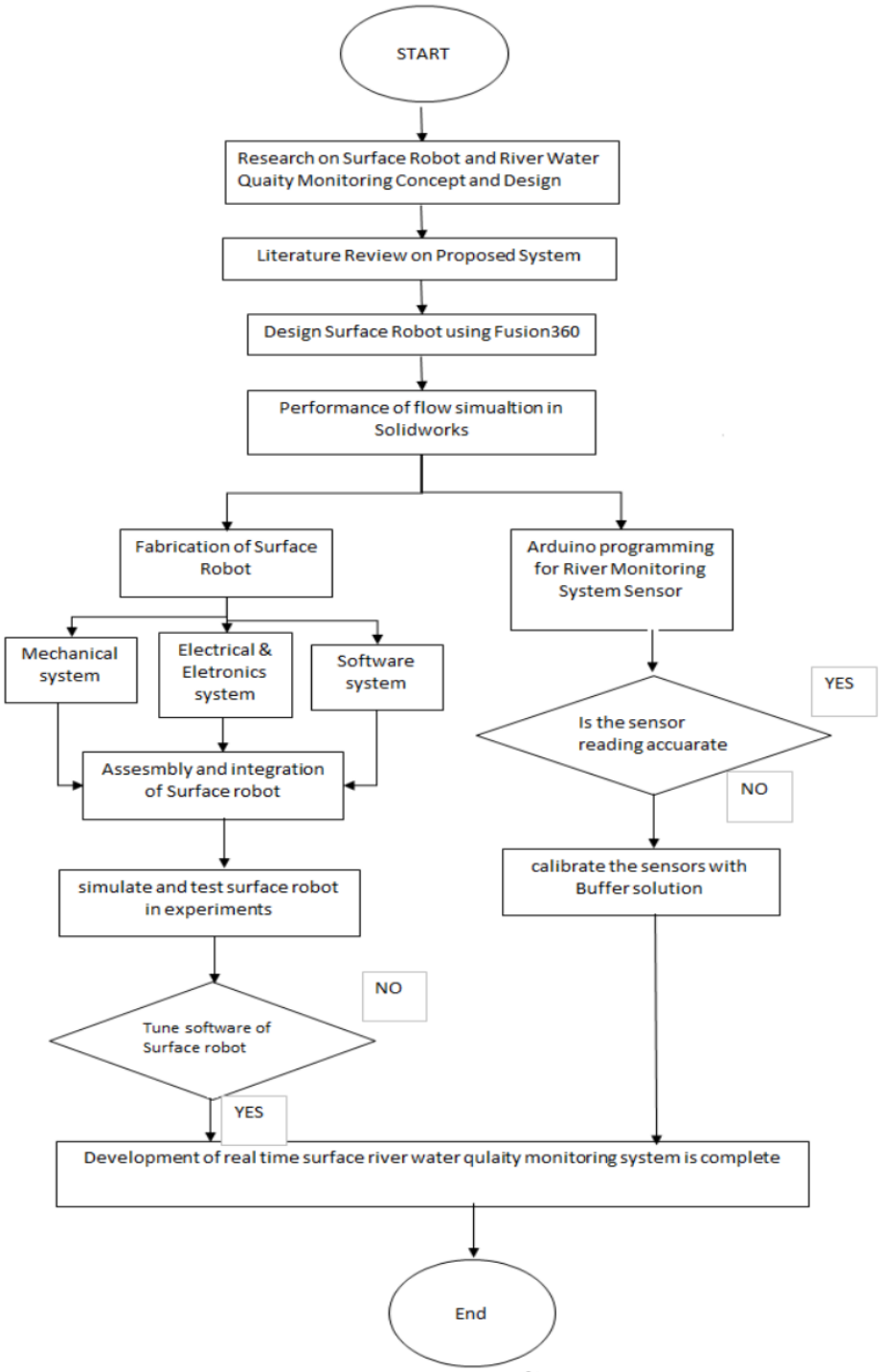

Figure 1. Project Flow Chart

RESULTS AND DISCUSSION

Results Unmanned Surface Robot Design Using Fusion 360

The catamaran-style robot's boat and structure were designed using Fusion 360. A Surface Boat's Fusion 360 design entails building a thorough 3D model that precisely depicts the boat's components, construction and functionality. Blender 360. The shaping of the hull, which consists of two parallel hulls joined by a deck or crossbeam, is the first step in the design process. The designer can design the required catamaran shape using Fusion 360's modelling tools, taking into mind elements like stability, hydrodynamics and aesthetics. To obtain the necessary performance characteristics, the programme enables precise modifications of dimensions, angles and curves. Fusion 360 makes it easier to create thorough documentation and drawings for the surface robot. To facilitate the building and manufacturing processes, this involves creating assembly instructions, exploded views and dimensions. Figure 2 displays the surface robot in an exploded view.

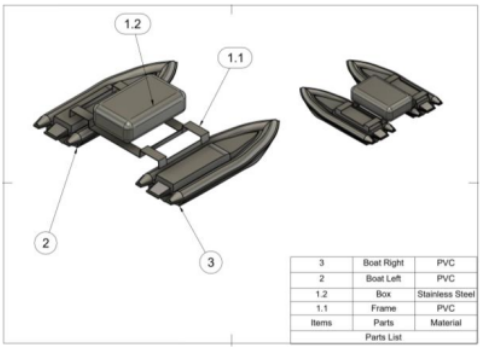

Figure 1. Exploded View of Surface Boat

According to Figure 2, the surface robot is shaped like a catamaran-style boat. For added buoyancy, both sides have twin hulls. Underframes connect the two hulls and offer room for sensor installation. Two thrusters are on the surface robot. The surface robot has the following dimensions: The boat's overall dimensions are 809mm in length, 718.24mm in width and 223.51mm in height. The surface boat's isometric measurements are shown in Figure 3.

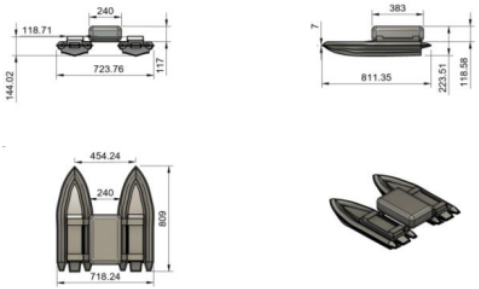

Figure 2. Isometric Measurement of Surface Boat

Circuit Design for River Monitoring System Sensor

Figure 4 shows the circuit diagram of river water quality monitoring system. The system consists of sensors that measure the pH level, TDS level and temperature of the river water. These sensors are connected to a microcontroller board such as Arduino or Raspberry Pi, which acts as the central processing unit. To ensure stable power supply, a step-down buck converter is used to regulate the voltage if needed. To transmit the collected data to a base station, a telemetry module is employed. This module establishes a communication link between the remote monitoring system and the base station. It is connected to the microcontroller board using the appropriate communication interface. The telemetry module converts the sensor readings into digital data and formats it according to the chosen communication protocol. The data packets containing the sensor readings are then sent via the telemetry module to the base station. At the base station, the transmitted data is received using a compatible telemetry module. The received data packets are processed to extract the sensor readings for further analysis.

To integrate the system with the Blynk IoT cloud, an account is created on the Blynk platform, and a new project is set up. Widgets such as gauges, graphs and buttons are added in the Blynk app to visualize and interact with the sensor data. An authentication token is generated for the Blynk project to establish a connection with the Blynk IoT cloud. The code is implemented on the microcontroller board to read the sensor data, format it and send it to the base station via the telemetry module. The Blynk library is used to integrate the Blynk IoT cloud into the code, enabling the transmission of sensor data. The data is sent to the Blynk IoT cloud using the generated authentication token. With the system set up, the Blynk app can be accessed on a mobile

device to connect to the Blynk IoT cloud. The sensor data is available in the app and the added widgets allow users to visualize and interact with the data. The pH level, TDS level and temperature of the river water can be monitored in real-time through the Blynk app.

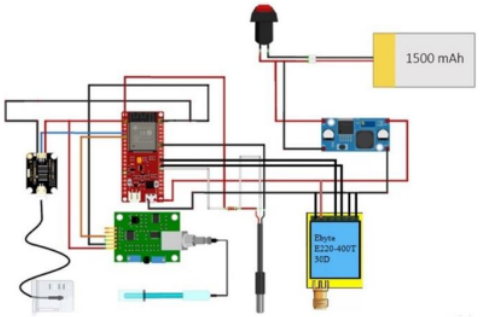

Figure 4. Circuit Diagram of River Water Quality Monitoring Sensors

Hardware Design of Unmanned Surface Robot

Figure 5 shows the finished hardware design of the surface robot. The mass of the surface robot when its empty is 1.65kg. The choice of material for the boat is PVC and the material chosen for the frame is Stainless Steel. Due to its light weight, toughness and corrosion resistance, PVC is a common material for the boat and box construction. It provides superior structural strength while keeping the vehicle's overall weight low. The speed, agility and fuel efficiency of the surface vehicle are all improved by its lightweight design. Boat frame is made of stainless steel because of its great strength, resistance to corrosion and durability. It ensures the vehicle can endure a variety of operating circumstances and outside forces by providing stability and structural support to important portions of the frame. Due to its superior corrosion resistance, stainless steel is especially well suited for applications where the frame will be exposed to seawater or harsh maritime environments. The boat included buoyancy chambers within each hull. These chambers are sealed compartments that provide additional buoyancy and help maintain the vehicle's floatability even in the event of damage or water ingress. They enhance the overall safety and stability of the surface vehicle.

Figure 5. Hardware Design of Unmanned Surface Robot

Experiment 1: Flysky FS-IA6B Receiver Range Test

The experiment conducted was a range test for the Flysky FS-IA6B receiver, aiming to determine the maximum distance at which the receiver can successfully receive signals from the controller. The test was carried out in different scenarios involving varying distances and obstacles between the receiver and the transmitter (controller). The experiment started at a distance of 50 meters, with the receiver placed in a clear space. In this scenario, the receiver successfully connected to the transmitter, indicating that the signal was able to reach the receiver without any obstacles present. Next, the experiment introduced obstacles between the receiver and transmitter, still at a distance of 50 meters. The receiver remained connected in this scenario as well, indicating that the signal was able to penetrate the obstacles and reach the receiver. The experiment then proceeded to test the range at a greater distance of 100 meters, while maintaining the obstacles between the receiver and transmitter. In this case, the receiver became disconnected, suggesting that the signal was no longer able to overcome the obstacles and reach the receiver at this distance.

To further investigate the range, the test was continued at a distance of 200 meters. Surprisingly, the receiver was able to connect successfully at this distance, even with the obstacles present. This suggests that the signal was able to reach the receiver despite the increased distance. Finally, the experiment pushed the range to 224 meters (line of sight),

without any obstacles between the receiver and transmitter. At this distance, the receiver became disconnected, indicating that the maximum range of the Flysky FS-IA6B receiver in clear line of sight conditions is 224 meters. Overall, the range test experiment demonstrated the maximum distance at which the receiver could receive signals from the controller. It showed that the receiver could successfully connect at distances up to 200 meters with obstacles present, but disconnected beyond that distance. However, in clear line of sight conditions, the receiver's maximum range was determined to be 224 meters. Table 4 indicates the FS-IA6B receiver range test.

Table **Error! No text of specified style in document.**. FS-IA6B Receiver Range Test Result

Distance (m)	Connectivity of Receiver on Clear Space	Connectivity of Receiver with Obstacles
50	Connected	Connected
60	Connected	Connected
70	Connected	Connected
100	Connected	Connected
200	Connected	Failsafe
224	Connected	Failsafe
226	Failsafe	Failsafe
300	Failsafe	Failsafe
400	Failsafe	Failsafe
500	Failsafe	Failsafe

Experiment 2: 433MHz Telemetry Range Test with Lora Module E220-400T30D

The experiment conducted aimed to determine the maximum distance at which the Lora module E220 could send and receive data to and from a base station. The test involved gradually increasing the distance between the transmitter and receiver while monitoring the ability to establish and maintain a connection. The experiment began at a distance of 50 meters, where both the transmitter and receiver were able to successfully transmit and receive signals. This indicated that the communication between the two devices was functioning properly within this range. The distance was then increased, and at 272 meters, an obstacle was introduced between the receiver and transmitter. As a result, the receiver and transmitter became disconnected, indicating that the obstacle obstructed the signal and prevented successful communication at this distance as shown in Table 5.

To further evaluate the range, the experiment continued without any obstacles between the transmitter and receiver. It was observed that the receiver remained connected even at 700 meters. This suggests that without any obstructions, the Lora module E220 could maintain a reliable connection over a considerable distance. The experiment eventually stopped at 800 meters. The decision to conclude the test at this distance was due to the availability of the testing area, specifically Ayer Keroh Lake. As the maximum distance without any obstacles that could be tested in this location was determined to be 800 meters, the experiment was concluded at that point. In summary, the experiment aimed to determine the maximum distance for data transmission using the Lora module E220. It was found that with obstacles present, the connection was lost at 272 meters. However, without any obstacles, the receiver remained connected up to a distance of 700 meters. The test was halted at 800 meters due to limitations in the available testing area.

Table 5. 433MHz Telemetry Range Test Result

Distance (m)	Connectivity of Receiver on Clear Space	Connectivity of Receiver with Obstacles
50	Connected	Connected
60	Connected	Connected
70	Connected	Connected
100	Connected	Connected
200	Connected	Connected
272	Connected	Failsafe
300	Connected	Failsafe
400	Connected	Failsafe
500	Connected	Failsafe
700	Connected	Failsafe
800	Connected	Failsafe

Experiment 3: pH Sensor and TDS Sensor Accuracy Calculation

The purpose of this experiment was to evaluate the accuracy of the pH sensor and the Total Dissolved Solids (TDS) sensor. It was observed that when the TDS sensor and the pH sensor were placed together, the pH sensor readings showed significant interference. The pH sensor readings increased by more than 17 pH units, which is an incorrect value. To quantify this interference, the experiment involved placing both sensors together in buffer solutions with known fixed pH values. Three different buffer solutions were used, with pH values of 4, 6.86 and 9.18. The ADC (Analog-to-Digital Converter) readings of the pH sensor were recorded while it was positioned alongside the TDS sensor in each buffer solution. The collected data was then tabulated in Table 6, and a linear graph was plotted using the pH sensor ADC readings as the independent variable (x-axis) and the corresponding pH values as the dependent variable (y-axis). Figure 6 represents this linear graph. By analyzing the plotted data, a linear equation was determined to represent the relationship between the pH sensor ADC readings

and the accurate pH values. The obtained linear equation was y = -5.7062x + 17.505, where y represents the pH reading.

To enhance the accuracy of the pH sensor readings, this linear equation was incorporated into the ADC code of the pH sensor. By modifying the Arduino coding accordingly, the pH sensor's readings could be adjusted to compensate for the interference caused by the TDS sensor. After editing the Arduino code, the accuracy of the pH sensor was tested once again using the buffer solutions. The aim was to verify whether the modified coding, incorporating the linear equation, improved the accuracy of the pH sensor readings. In summary, the experiment assessed the interference between the pH sensor and the TDS sensor and identified a significant increase in pH sensor readings when the two sensors were placed together. By establishing a linear equation that accounted for this interference, the accuracy of the pH sensor was enhanced. The modified Arduino code incorporating this equation enabled more accurate pH readings when tested with buffer solutions. The accuracy of pH and TDS sensor is shown in the Table 7.

Table 6. pH Sensor ADC Reading

pH Reading	Average ADC Output from pH Sensor
4	2.368
6.86	1.867
9.18	1.4596

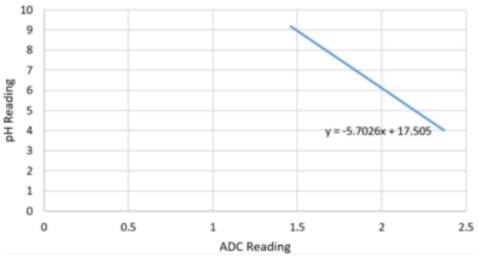

Figure 6. Linear Graph for pH Sensor ADC Reading

Table 7. pH Sensor and TDS Sensor Accuracy Table

Buffer Solution pH Value (pH)	pH Measured from the pH Sensor (pH)	pH Sensor Error	TDS Calibration Solution Value (PPT)	TDS Measure from the Sensor (PPT)	TDS Sensor Error
4.01	5.2	0.296	35	40ppt	0.1428
6.86	7.1	0.035	-	-	-
9.18	9.5	0.034	-	-	-

Experiment 4: Payload Test

A payload test for a surface robot involves assessing its capacity to carry and transport additional weight or cargo, while maintaining its stability and performance. This test helps determine the boat's maximum payload capacity and ensures that it can handle the intended load without compromising its maneuverability or safety. To carry out the payload test, the surface robot is measures without any additional mass in it. Then, measure the original submerged distance of the surface robot. Then, add in materials to increase the mass inside the surface boat measure the submerged percentage of the surface robot. Continue this process until the water starts to leak into the boat. Table 8 shows the original mass of the boat is 2.5kg. The maximum weight till the water starts to leak into the boat is 11.85kg where the boat is 70% submerged into the water.

Table 8. Payload Test Result

Mass	Submerged Percentage	Water Getting in
Original mass of surface robot with frame: 2500g	10%	NO
2850	25%	NO
3850g	35%	NO
5850g	40%	NO
7850	50%	NO
9850	65%	NO
11850	70%	YES

Experiment 5: Turning Test

The turning test conducted on the surface robot aimed to measure the time taken for the robot to complete a 360-degree circle and a 180-degree circle. This test helps assess the maneuverability and agility of the robot in turning movements. Table 8 presents the results of the test for a 360-degree circle. The test was conducted three times, and the time taken for each trial was recorded. To determine the average time, the three recorded times were added together and the sum was divided by three. The average time to complete a 360-degree circle was found to be 3.25 seconds. Similarly, Table 9 displays the results for the test conducted for a 180-degree circle. The test was also conducted three times, and the time taken for each trial was recorded. The average time was calculated by summing the three recorded times and dividing the sum by three. The average time to complete a 180-degree circle was determined to be 1.07 seconds. By conducting these turning tests and calculating the

average times, the surface robot's performance in completing 360-degree and 180-degree circles can be evaluated. The shorter the average time, the quicker the robot can execute turns, indicating higher maneuverability and agility. The turning test for the surface robot involved measuring the time taken to complete a 360-degree circle and a 180-degree circle. By conducting multiple trials and calculating average times, the average time for completing each type of turn was determined. In this case, the robot took an average of 3.25 seconds to complete a 360-degree circle and 1.07 seconds to complete a 180-degree circle. These times provide insights into the robot's turning capabilities and overall maneuverability. Figure 7 shows the turning test result from mission planner data logger which shows average of 360 degrees turn and time taken.

Table 9. Time taken to complete 360 Degrees

Degree of Turning (Degrees)	Time Taken (s)
359.72	3.3
359.99	3.28
356.78	3.18
Average : 358.83	3.25

Table 10. Time taken to Complete 180 Degrees

Degree of Turning (Degrees)	Time Taken (s)
182.3	1.1
178.9	1.13
179.99	1
Average : 180.39	1.07

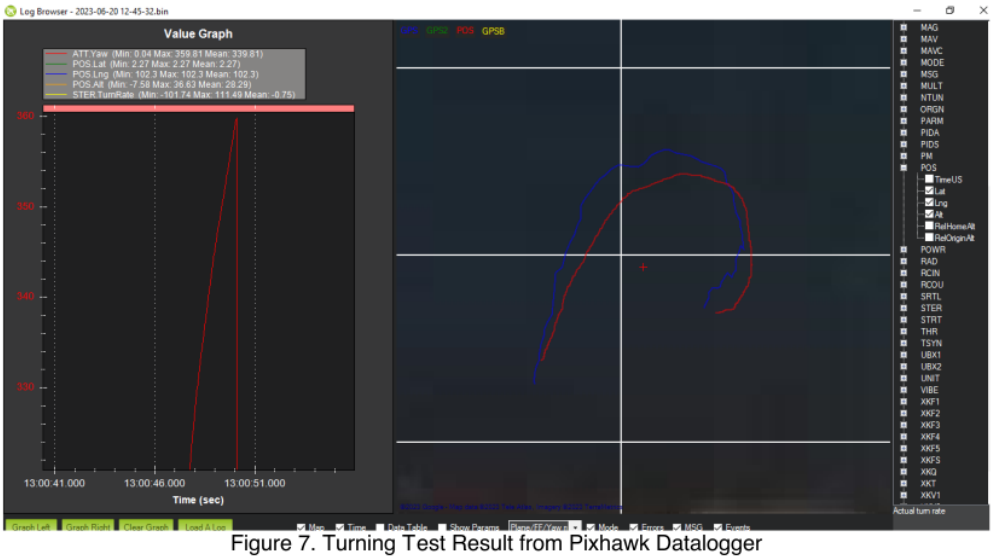

Figure 7. Turning Test Result from Pixhawk Datalogger

Sensor Reading from Ayer Keroh Lake

Figure 8 displays a graph representing the readings taken from Ayer Keroh Lake during testing. The testing was conducted from the lakebed to the middle of the lake, allowing for observations of various water parameters. At the beginning of the test, the TDS (Total Dissolved Solids) sensor reading recorded a value of 68 ppm (parts per million). This reading corresponds to an electrical conductivity (EC) of 138 μs/cm (micro-siemens per centimeter). Additionally, the pH reading was recorded at 11 units, indicating that the water was alkaline. As the surface robot reached the middle of the lake, the TDS reading increased to 130 ppm and the EC value rose to 260 μs/cm. This suggests that the concentration of dissolved solids in the water had significantly increased in comparison to the starting point. Furthermore, the pH reading also experienced an increase, reaching a value of 12.65. This indicates a further shift towards alkalinity in the water.

Towards the end of the testing period, both the TDS and pH readings remained consistently high. This implies that the water in Ayer Keroh Lake had a substantial concentration of dissolved solids and maintained an alkaline pH level throughout the tested area. The information provided by the graph helps to assess the water quality in Ayer Keroh Lake. The increasing TDS and EC readings suggest a higher concentration of dissolved solids, which could include various minerals, salts or other organic and inorganic substances. The elevated pH reading indicates the water's alkaline nature. Figure 9 shows the

notification received from Blynk application when the data reading exceeds the limits set.

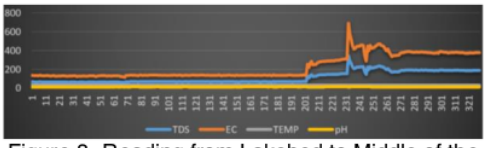

Figure 8. Reading from Lakebed to Middle of the Lake

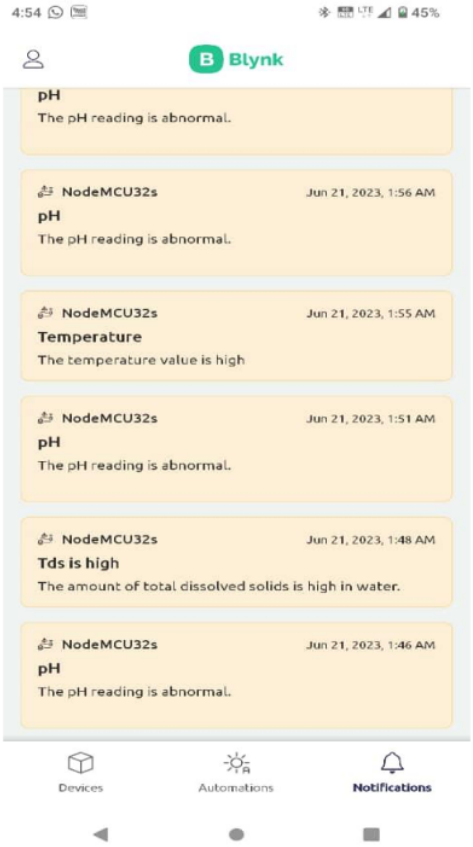

Figure 9. Notification Received from Blynk Application When the Reading Is Abnormal

Pixhawk Autopilot Result

Figure 10 and Figure 11 depict the results of waypoint missions carried out using a surface robot or drone. These missions involved navigating through a series of predetermined waypoints. However, the figures indicate that the waypoint missions were inaccurate, potentially deviating from the desired path. To address this issue and improve the accuracy of the waypoint missions, the addition of a PID (Proportional-Integral-Derivative) system filter in Mission Planner is suggested. A PID system is a control loop feedback mechanism commonly used in robotics and automation to improve stability and accuracy. By implementing a PID system filter, the surface robot or drone can benefit from the improvements of proportional control. The proportional component of the PID system helps adjust the robot's navigation based on the difference between the desired waypoint location and its current position. It provides a corrective signal that is proportional to the error, helping steer the robot back on track towards the waypoints. The integral component of the PID system takes into account the accumulated error over time. It continuously adjusts the navigation by considering the historical error and applying corrective measures. This helps to address any steady-state errors or biases that may arise during the mission. The derivative component of the PID system considers the rate of change of the error. It helps provide damping and anticipates any sudden changes in the robot's position. This component aids in smoothing out the robot's movements and reducing overshoot or oscillations, resulting in more accurate navigation between waypoints.

By incorporating these PID control mechanisms into the Mission Planner software, the accuracy of the waypoint missions can be significantly enhanced. The PID system filter continuously analyzes the robot's position in relation to the desired waypoints and adjusts its navigation accordingly, ensuring precise adherence to the intended path. In summary, Figures 10 and 11 illustrate the need for increased accuracy in waypoint missions carried out by a surface robot or drone. The addition of a PID system filter in Mission Planner is suggested to improve the robot's navigation capabilities. The PID system provides proportional, integral and derivative control mechanisms to correct errors, compensate for biases, and smooth out movements, resulting in more accurate and reliable navigation between waypoints.

Figure 10. Autopilot Test with Three Waypoints Mission

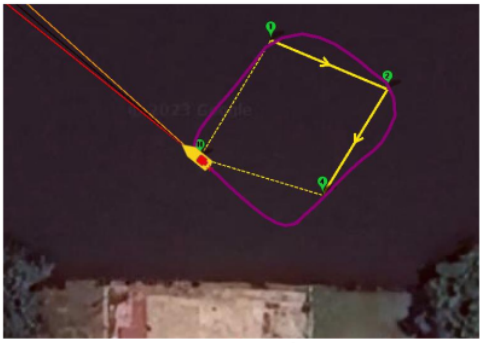

Figure 11. Autopilot Test with Four Waypoints Mission

CONCLUSION

The range tests conducted in experiments one and two were crucial in establishing the operational limits of the surface robot. By progressively increasing the distance from the control station while ensuring continuous communication and control, the team successfully determined the maximum range at which the robot could effectively operate. This information provides valuable insight for planning and executing river water quality monitoring missions. Experiment three focused on enhancing the accuracy of the water quality monitoring sensors installed on the surface robot. Through calibration and fine-tuning of sensor parameters, the team achieved higher accuracy readings by the end of the experiment. This improvement in accuracy validates the fulfillment of objective three, highlighting the successful development of a surface robot capable of providing more precise water quality data.

ACKNOWLEDGMENT

We wish to express our gratitude to the honorab Universiti Teknikal Malaysia Melaka (UTeM) for sponsoring t s work under grant no. PJP/2022/FKE/S01858. Special appreciation and gratitude especially for Faculty o echnology and Electrical Engineering (FTKE) and Underwater Technology Research Group (UTeRG), Center for Robotics and Industrial Automation (CERIA) for supporting this research.

real

ORIGINALITY REPORT

7%	5%	5%	4%
SIMILARITY INDEX	INTERNET SOURCES	PUBLICATIONS	STUDENT PAPERS

PRIMARY SOURCES

1	Submitted to Universitas Diponegoro Student Paper	2%
2	www.researchgate.net Internet Source	1%
3	nopr.niscair.res.in Internet Source	1%
4	repository.unsri.ac.id Internet Source	<1%
5	"Proceedings of the 11th National Technical Seminar on Unmanned System Technology 2019", Springer Science and Business Media LLC, 2021 Publication	<1%
6	Ton Duc Thang University Publication	<1%
7	Submitted to Universiti Teknologi Malaysia Student Paper	<1%
8	media.neliti.com Internet Source	<1%

9	Sahbi Khanfir, Kazuhiko Hasegawa, Vishwanath Nagarajan, Kouichi Shouji, Seung Keon Lee. "Manoeuvring characteristics of twin-rudder systems: rudder-hull interaction effect on the manoeuvrability of twin-rudder ships", Journal of Marine Science and Technology, 2011 Publication	<1 %
10	Submitted to Canterbury Christ Church University Student Paper	<1 %
11	Hofmann, Angie. "Scientific Writing and Communication", Scientific Writing and Communication, 2022 Publication	<1 %
12	cyberleninka.org Internet Source	<1 %
13	Submitted to universititeknologimara Student Paper	<1 %
14	Submitted to Universiti Teknikal Malaysia Melaka Student Paper	<1 %
15	www.hindawi.com Internet Source	<1 %
16	Donghoon Kang. "Mathematical model of single-propeller twin-rudder ship", Journal of	<1 %

Marine Science and Technology, 08/2008
Publication

17	Mohamad Haniff Harun, Shahrum Shah Abdullah, Mohd Shahrieel Mohd Aras, Mohd Bazli Bahar. "Sensor Fusion Technology for Unmanned Autonomous Vehicles (UAV): A Review of Methods and Applications", 2022 IEEE 9th International Conference on Underwater System Technology: Theory and Applications (USYS), 2022 Publication	<1 %
18	www.ncbi.nlm.nih.gov Internet Source	<1 %
19	Yong Li, Liqiao Tian, Wenkai Li, Jian Li, Anna Wei, Sen Li, Ruqing Tong. "Design and Experiments of a Water Color Remote Sensing-Oriented Unmanned Surface Vehicle", Sensors, 2020 Publication	<1 %

Exclude quotes	Off	Exclude matches	Off
Exclude bibliography	Off		